Qualitative stability and synchronicity analysis of power network models in port-Hamiltonian form

Cite as: Chaos **28**, 101102 (2018); https://doi.org/10.1063/1.5054850
Submitted: 04 September 2018 . Accepted: 01 October 2018 . Published Online: 18 October 2018

Volker Mehrmann, Riccardo Morandin, Simona Olmi, and Eckehard Schöll

Qualitative stability and synchronicity analysis of power network models in port-Hamiltonian form

Volker Mehrmann,[1,a)] Riccardo Morandin,[1,b)] Simona Olmi,[2,3,4,c)] and Eckehard Schöll[2,d)]
[1]*Institut für Mathematik MA 4-5, TU Berlin, Str. des 17. Juni 136, D-10623 Berlin, Germany*
[2]*Institut für Theoretische Physik, Sekr. EW 7-1, TU Berlin, Hardenbergstr. 36, D-10623 Berlin, Germany*
[3]*INRIA Sophia Antipolis Méditerranée, 2004 Route des Lucioles, 06902 Valbonne, France*
[4]*CNR—Consiglio Nazionale delle Ricerche—Istituto dei Sistemi Complessi, 50019 Sesto Fiorentino, Italy*

(Received 4 September 2018; accepted 1 October 2018; published online 18 October 2018)

In view of highly decentralized and diversified power generation concepts, in particular with renewable energies, the analysis and control of the stability and the synchronization of power networks is an important topic that requires different levels of modeling detail for different tasks. A frequently used qualitative approach relies on simplified nonlinear network models like the Kuramoto model with inertia. The usual formulation in the form of a system of coupled ordinary differential equations is not always adequate. We present a new energy-based formulation of the Kuramoto model with inertia as a polynomial port-Hamiltonian system of differential-algebraic equations, with a quadratic Hamiltonian function including a generalized order parameter. This leads to a robust representation of the system with respect to disturbances: it encodes the underlying physics, such as the dissipation inequality or the deviation from synchronicity, directly in the structure of the equations, and it explicitly displays all possible constraints and allows for robust simulation methods. The model is immersed into a system of model hierarchies that will be helpful for applying adaptive simulations in future works. We illustrate the advantages of the modified modeling approach with analytics and numerical results. *Published by AIP Publishing.* https://doi.org/10.1063/1.5054850

To reach the goal of temperature reduction to limit the climate change, as stipulated at the Paris Conference in 2015, it is necessary to integrate renewable energy sources into the existing power networks. Wind and solar power are the most promising ones, but the integration into the electric power grid remains an enormous challenge due to their variability that requires storage facilities, back-up plants, and accurate control processing. The current approach to describe the dynamics of power grids in terms of simplified nonlinear models, like the Kuramoto model with inertia, may not be appropriate when different control and optimization tasks are needed to be addressed. Under this aspect, we present a new energy-based formulation of the Kuramoto model with inertia that allows for an easy extension if further effects have to be included and higher fidelity is required for qualitative analysis. We illustrate the new modeling approach with analytic results and numerical simulations carried out for a semi-realistic model of the Italian grid and indicate how this approach can be generalized to models of finer granularity.

I. INTRODUCTION

The increasing usage of renewable energy sources, such as wind and solar power, and the decentralization of power generation make the stability and synchronization control of modern power systems very difficult. To address different control and optimization tasks, there are different modeling approaches for the various components of power networks; we will briefly present a model hierarchy for synchronous generators and transmission lines. The simplest model in the hierarchy is the Kuramoto model with inertia, which is often used for a qualitative analysis of the network behavior.[1,2]

The usual formulation of the Kuramoto model with inertia in the form of a coupled system of ordinary differential equations as in Refs. 1–7 is, however, not always appropriate, because physical properties like the conservation of energy and momentum are only implicitly represented in the equations, and thus, in numerical simulation or control, they may be violated and lead to un-physical behavior. To prevent this, we present a new energy-based formulation of the Kuramoto model with inertia as port-Hamiltonian system of differential-algebraic equations (pHDAEs). This formulation is closely related to the one in Refs. 8 and 9, but it uses a change of variables, similar to Ref. 10, to turn the system into a polynomial system with quadratic Hamiltonian.

Port-Hamiltonian (pH) systems (Refs 11–13) have become a paradigm for multi-physics systems modeling incorporated in automated modeling frameworks such as 20-SIM http://www.20sim.com/; see Ref. 14. To include interface conditions or constraints, in Refs. 15 and 16, ordinary pH systems have been extended to *port-Hamiltonian DAEs* (pHDAEs). Although the discussed systems are nonlinear, we present here, for simplicity, the definition in a linear time-varying form, which describes the local behavior in the neighborhood of solutions; see Ref. 16 for the nonlinear version. Denote for a compact interval $\mathbb{I} \subseteq \mathbb{R}$ by $C^j(\mathbb{I} \times \mathbb{R}^n, \mathbb{R}^m)$ the set of j-times continuously differentiable functions from $\mathbb{I} \times \mathbb{R}^n$ to $\mathbb{R}^m$.

a)Electronic mail: mehrmann@math.tu-berlin.de
b)Electronic mail: morandin@math.tu-berlin.de
c)Electronic mail: simona.olmi@inria.fr
d)Electronic mail: schoell@physik.tu-berlin.de

Definition 1. A linear variable coefficient system

$$\begin{aligned} E\dot{x} &= [(J-R)Q - ET]\,x + (B-P)u, \\ y &= (B+P)^T Qx + (S+N)u, \end{aligned} \tag{1}$$

with $E, Q \in C^1(\mathbb{I}\times\mathbb{R}^n, \mathbb{R}^{n,n})$, $J, R, T \in C^0(\mathbb{I}\times\mathbb{R}^n, \mathbb{R}^{n,n})$, $B, P \in C^0(\mathbb{I}\times\mathbb{R}^n, \mathbb{R}^{n,m})$, $S, N \in C^0(\mathbb{I}\times\mathbb{R}^n, \mathbb{R}^{m,m})$, and $S = S^T$, $N = -N^T$ is called *port-Hamiltonian differential-algebraic system (pHDAE)* if

(i) Along all solutions $x : \mathbb{I} \to \mathbb{R}^n$ of (1), we have

$$(Q^TE)[t, x(t)] = (E^TQ)[t, x(t)] \in C^1(\mathbb{I}, \mathbb{R}^{n,n})$$

and for all $t \in \mathbb{I}$, we have

$$\begin{aligned} \frac{d}{dt}\big\{(Q^TE)[t, x(t)]\big\} = \big[&Q^T(ET - JQ) \\ &+ (ET - JQ)^TQ\big][t, x(t)]; \end{aligned}$$

(ii) the *Hamiltonian* function $\mathcal{H} = \frac{1}{2}x^T[(Q^TE)(t, x)]x \in C^1(\mathbb{I}\times\mathbb{R}^n, \mathbb{R})$ satisfies $\mathcal{H}[t, x(t)] \geq h_0$ uniformly for some $h_0 \in \mathbb{R}$, all $t \in \mathbb{I}$ and all solutions $x(t)$ of (1);

(iii) for all $t \in \mathbb{I}$, $W = W^T \geq 0$, where

$$W := \begin{bmatrix} Q^TRQ & Q^TP \\ P^TQ & S \end{bmatrix} \in C^0(\mathbb{I}\times\mathbb{R}^n, \mathbb{R}^{n+m,n+m}). \tag{2}$$

pHDAEs satisfy the *dissipation inequality*

$$\mathcal{H}[t_1, x(t_1)] - \mathcal{H}[t_0, x(t_0)] \leq \int_{t_0}^{t_1} y(t)^T u(t)\, dt, \tag{3}$$

which shows that (1) is a *passive* system (see Ref. 17), and since $\mathcal{H}(x)$ defines a Lyapunov function, pH systems are implicitly Lyapunov stable. An advantage of pHDAEs in the context of power system modeling is that they are closed under *power-conserving interconnection*, which allows one to build-up models in a modularized way (see Ref. 18), and Galerkin projection (see Ref. 19), which allows systematic discretization and model reduction.

II. MODEL HIERARCHIES FOR POWER NETWORKS

A power network consists of many different types of components, e.g., the synchronous generators, the loads, and the transmission lines. Each of these components can be modeled with a different degree of fidelity, depending on the state of the system, the dynamics of the network, the task that has to be completed, the accuracy requirements, or the allowed computation time. The innate modularity of pH systems allows one to interconnect different components of the network while retaining energy-consistency, even between different models in the hierarchy, and can be easily exploited by automated modeling frameworks. It can also be combined with structure-preserving model reduction methods that allow one to speed up computations while retaining qualitative behavior.

A detailed synchronous generator model including the electromagnetic phenomena internal to the generator (see, e.g., Refs. 9 and 20) can be drastically simplified by neglecting the dynamics of the magnetic variables, leading to the *swing equation*,[9] which can be modeled with different accuracy (see, e.g., Ref. 21).

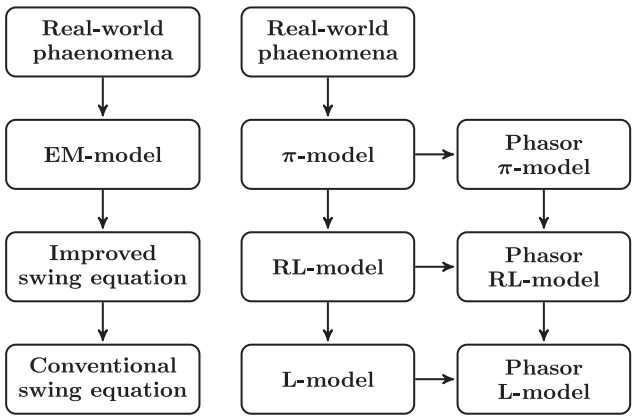

FIG. 1. Model hierarchies for synchronous generators (on the left) and transmission lines (on the right).

Also, the model of a transmission line, represented as a circuit with resistive, inductive, and capacitive components (see, e.g., Refs. 2 and 20) can be further simplified: both the shunt capacitance and the series resistance are often negligible when compared with the inductance, and when assuming steady-state, the phasor model can be used, substituting the equations for the current through the transmission line by a linear relation. See Fig. 1 for a summary of the two *model hierarchies*.

For the purpose of this paper, we consider a power network consisting of n synchronous generators, connected through transmission lines, using the conventional swing equation for the synchronous generators, and the phasor L-model for the transmission lines. The resulting system [see Ref. 9 (subsection 6.2)] can be written as

$$m_j\dot{\omega}_j = -d_j\omega_j + \sum_{k=1}^{n} g_{jk}\sin(\theta_k - \theta_j) + P_j, \tag{4}$$

for $j = 1, \ldots, n$, where θ_j is the phase shift, $\omega_j = \dot{\theta}_j$ is the deviation from a given (nominal) frequency Ω, $m_j > 0$ is the inertia, $d_j > 0$ is the damping constant, $P_j \in \mathbb{R}$ is the power balance of the j-th generator, $g_{jk} = B_{jk}E_jE_k \geq 0$, where B_{jk} is the susceptance of the transmission line between the j-th and k-th node, and E_j, E_k are the respective amplitudes of the voltage potentials (assumed constant). Note that we allow the power balance to be negative, so that a generator can also be interpreted as a load. This model can be written as an $m+n$-dimensional ordinary port-Hamiltonian system (see Refs. 8 and 9) with variables $q = [\theta_k - \theta_j] \in \mathbb{R}^m$ (indexed as the edges of the network graph) and $p = [m_j\omega_j] \in \mathbb{R}^n$:

$$\begin{aligned} \dot{q} &= \mathcal{A}^T\omega, \\ M\dot{\omega} &= -D\omega - \mathcal{A}\Gamma\sin q + P, \end{aligned} \tag{5}$$

with Hamiltonian

$$\mathcal{H}(q, p) := \frac{1}{2}p^TM^{-1}p - \mathbf{1}^T\Gamma\cos q, \tag{6}$$

where $M = \mathrm{diag}(m_j)$, $D = \mathrm{diag}(d_j) \in \mathbb{R}^{n,n}$, $\Gamma = \mathrm{diag}[g_{jk}] \in \mathbb{R}^{m,m}$, $P = [P_j] \in \mathbb{R}^n$, $\mathcal{A} \in \mathbb{R}^{n,m}$ is the incidence matrix of the graph, and $\mathbf{1}$ is the vector of all ones.

System (4) is a generalization of the canonical second-order Kuramoto model with inertia, which consists of a

system of n fully-coupled oscillators satisfying

$$m_j\ddot{\theta}_j + d_j\dot{\theta}_j = \Omega_j + K\sum_{k=1}^{n}\sin(\theta_k - \theta_j), \tag{7}$$

for $j = 1,\dots,n$, where θ_j, m_j, d_j are as before, Ω_j are the natural frequencies, and $K > 0$ is the coupling constant of the system. We will refer to system (4) as the *generalized Kuramoto model* (GKM). To study qualitatively the synchronization of oscillatory networks, typically the *complex order parameter* (COP)

$$re^{i\phi} := \frac{1}{n}\sum_{j=1}^{n} e^{i\theta_j} \in \{z \in \mathbb{C} : |z| \le 1\}$$

is used where $r = 1$ when the system is in a fully synchronized state and 0 when it is completely desynchronized.

III. THE GENERALIZED ORDER PARAMETER

While the COP is linked to the fully-coupled canonical Kuramoto model with inertia, (see Ref. 3) in the case of sparse networks, it can show weird behavior (see, e.g., Fig. 3 or Ref. 22), because it does not take the topology of the system into account, and so it fails to capture well the transitions in the partially phase locked regime. To address this problem, we introduce a *generalized order parameter* (GOP) that applies to the GKM and is consistent with the COP. Treating (7) as a special case of (4) with a complete graph and $g_{jk} \equiv K$, we can write

$$r^2 = |re^{i\phi}|^2 = \frac{1}{n^2}\sum_{j,k} e^{i(\theta_k-\theta_j)} = \frac{1}{n^2}\sum_{j,k}\cos(\theta_k-\theta_j)$$
$$= \frac{2}{n^2}\sum_{j<k}\cos(\theta_k-\theta_j) + \frac{1}{n} = \frac{2}{Kn^2}\mathbf{1}^T\Gamma\cos q + \frac{1}{n};$$

thus, in this case, $\mathbf{1}^T\Gamma\cos q = \frac{1}{2}Kn^2r^2 - \frac{1}{n}$. Since the pH formulation does not change if we add a constant to its Hamiltonian, we can replace (6) with

$$\mathcal{H}_1(q,p) := \frac{1}{2}p^TM^{-1}p + \frac{1}{2}Kn^2[1 - r(q)^2] \ge 0. \tag{8}$$

To extend the definition of the order parameter to the general case, without losing its connection to the Hamiltonian, we define the GOP $\xi(q) := a\mathbf{1}^T\Gamma\cos q + b$ for some network-dependent constants $a, b \in \mathbb{R}$, which should satisfy the following conditions:

(1) In the case of system (7), we have $\xi(q) \equiv r^2(q)$;
(2) the maximum value of $\xi(q)$ is 1, and it corresponds to the fully synchronized state;
(3) the minimum value of $\xi(q)$ is greater or equal to a fixed value $\xi_0 \in \mathbb{R}$.

We can restate these conditions in terms of a and b:

(1) Since in (7) we have $r^2 = \frac{2}{Kn^2}\mathbf{1}^T\Gamma\cos q + \frac{1}{n}$, for that network we must have $a = 2/Kn^2$ and $b = 1/n$.
(2) The fully synchronized state $\bar{q}$ corresponds to $\cos\bar{q} = \mathbf{1}$ and $\xi(\bar{q}) = a\mathbf{1}^T\Gamma\mathbf{1} + b$, so $\xi(\bar{q})$ is the maximum if and only if $a \ge 0$, and it is equal to 1 if and only if $b = 1 - a\mathbf{1}^T\Gamma\mathbf{1}$.
(3) If we assume (2), then $\xi(q) \ge -a\mathbf{1}^T\Gamma\mathbf{1} + b = 2b - 1$ for all q. Whether this value can actually be reached depends on the network, however, there is no clear general formula for $\min_q \xi(q)$. In any case, $b \ge \frac{1+\xi_0}{2}$ is sufficient to imply condition (3).

Using the given freedom, we choose $b = 1/n$ and $a = (n-1)/(n\mathbf{1}^T\Gamma\mathbf{1})$, so that conditions (1)–(3) are satisfied with $\xi_0 = -1 + \frac{1}{n}$, in particular $\xi(q) \in (-1, 1]$. Note that typically we will have $\xi(q) > 0$. We can express the Hamiltonian (6) in terms of the GOP. Changing $\mathcal{H}(q,p)$ again by an additive constant, we obtain

$$\mathcal{H}_2(q,p) := \frac{1}{2}p^TM^{-1}p + \frac{n}{n-1}\mathbf{1}^T\Gamma\mathbf{1}[1 - \xi(q)] \tag{9}$$
$$= \frac{1}{2}p^TM^{-1}p - \mathbf{1}^T\Gamma\cos q + \mathbf{1}^T\Gamma\mathbf{1}, \tag{10}$$

which has 0 as its minimum. We will show in Sec. V that the GOP $\xi(q)$ behaves better than the ordinary COP, especially for sparsely coupled networks. Note that a similar GOP has been formulated simultaneously to Ref. 23 in Ref. 22; however, it has not been related to a pH formulation nor applied to power grid networks.

IV. A NEW PHDAE FORMULATION FOR THE GKM

Similar to Ref. 10, we introduce $(\rho,\sigma) := (\cos\theta, \sin\theta)$, viewed componentwise, and express (4) in $x = (\omega,\rho,\sigma)$. Using $g_{jk} = 0$ when there is no edge connecting the j-th and k-th node, and introducing again $P = [P_j]$ in $\mathbb{R}^n$, $D = \mathrm{diag}(d_j)$, and $G = [g_{jk}]$ in $\mathbb{R}^{n,n}$, and the matrix functions $D_\rho = \mathrm{diag}(\rho_j)$, $D_\sigma = \mathrm{diag}(\sigma_j)$ with values in $\mathbb{R}^{n,n}$, we can write the GKM as

$$\begin{aligned} M\dot{\omega} &= -D\omega - D_\sigma G\rho + D_\rho G\sigma + P,\\ \dot{\rho} &= -D_\sigma\omega,\\ \dot{\sigma} &= D_\rho\omega. \end{aligned} \tag{11}$$

Since all terms with coefficients g_{jj} for $j = 1,\dots,n$ vanish in (11), we are free to choose g_{jj}; our choice is $g_{jj} = -\sum_{k\ne j} g_{jk}$, so that $G \le 0$. This can be interpreted as a pHDAE formulation $E\dot{x} = (J - R)Qx + Bu$ with $x = [\omega^T, \rho^T, \sigma^T]^T$, $u = P$, $E = \mathrm{diag}(M, I_n, I_n)$, $0 \le R = R^T = \mathrm{diag}(D, 0_n, 0_n)$, $Q = \mathrm{diag}(I_n, -G, -G)$,

$$J = -J^T = \begin{bmatrix} 0 & D_\sigma & -D_\rho \\ -D_\sigma & 0 & 0 \\ D_\rho & 0 & 0 \end{bmatrix}, \quad B = \begin{bmatrix} I \\ 0 \\ 0 \end{bmatrix},$$

and Hamiltonian function

$$\mathcal{H}_3(x) = \frac{1}{2}x^TQ^TEx = \frac{1}{2}\omega^TM\omega - \frac{1}{2}\rho^TG\rho - \frac{1}{2}\sigma^TG\sigma.$$

In particular, we have

$$\frac{1}{2}\rho^TG\rho + \frac{1}{2}\sigma^TG\sigma = \frac{1}{2}\sum_{j,k} g_{jk}\cos(\theta_k - \theta_j)$$
$$= \sum_{j<k} g_{jk}[\cos(\theta_k - \theta_j) - 1]$$
$$= \mathbf{1}^T\Gamma\cos q - \mathbf{1}^T\Gamma\mathbf{1},$$

so that $\mathcal{H}_3(x) = \mathcal{H}_2(q,p)$. This model has a larger state space than a modified version of (5) ($3n$ instead of $2n$), but it has several advantages.

- Using (ρ,σ) instead of θ as variables helps removing some redundancy from the state, without having to adjust $\theta_j \in [-\pi,\pi]$ numerically at each step. One can also consider a formulation with angles defined relative to a fixed oscillator; then, the zero state is the only fully synchronized state, and the matrix G becomes invertible (see Ref. 23).
- Although (11) is still a nonlinear system, it is now polynomial and has a quadratic Hamiltonian with respect to x; an advantage of this is, e.g., that, for $P = 0$ and $D = 0$, it can be integrated preserving $\mathcal{H}_2$ without discretization error (see Ref. 24).
- While (11) is still an ODE, we are allowed to add algebraic equations without losing the port-Hamiltonian structure. These could be, e.g., the relations linking the mechanical variables ω,ρ,σ to the electrical variables (voltage and currents), Kirchhoff's laws, or the implicit relation $\rho_j^2 + \sigma_j^2 = 1$.

Since we omitted the dependence of ρ and σ on θ, the variables ρ, σ implicitly need to satisfy $\rho_j^2 + \sigma_j^2 = 1$. Unfortunately, in numerical integrators for (11), such implicit relations are typically not preserved, due to discretization and roundoff errors.[25] To address this, we can add these conditions explicitly to the system, by introducing Lagrange multipliers $\mu = [\mu_j] \in \mathbb{R}^n$, adding the equation $0 = D_\rho\rho + D_\sigma\sigma - \mu$ to the system, and modifying correspondingly the matrices E, J, R, Q, B (see Ref. 23 for details). One must also make sure that the initial conditions are consistent and include $\mu = \mathbf{1}$. Employing geometric integrators helps one to preserve these conditions, as we show in Sec. V.

V. NUMERICAL RESULTS

In this section, we illustrate the advantages of our new pHDAE formulation by some numerical examples. We use a model of the Italian high-voltage (380 kV) power grid of $n = 127$ nodes, divided in 34 sources and 93 consumers, connected by 342 links, (see Ref. 26) and low average connectivity $n_c = 2.865$. See http://www.geni.org and https://www.entsoe.eu/map/Pages/no-webgl.html for a map and the data.

We use the GKM and assume for simplicity that each node has the same inertia and damping constant ($m_j = m = 6$ and $d_j = d = 1, j = 1,\dots,n$), and each transmission line has the same coupling coefficient, i.e., either $g_{jk} = K$ or $g_{jk} = 0$. To have a stable fully locked state as a possible solution of (4) (i.e., $\omega(t) \equiv 0$), it is necessary that $\sum_{j=1}^n P_j = 0$, which we get, e.g., by setting $P_j = -P_C = -1$ for all consumers, and $P_j = P_G = 2.7353$ for all generators. This corresponds to a Kuramoto model with inertia with perfectly balanced bimodal δ-distribution of the natural frequencies. Since in a real power grid the power of the generators (or consumers) will not have exactly the same values, we analyzed also the case where the P_j are chosen as random variables with distribution given by the superposition of two almost non-overlapping Gaussian distributions. See Ref. 23 for further computational results.

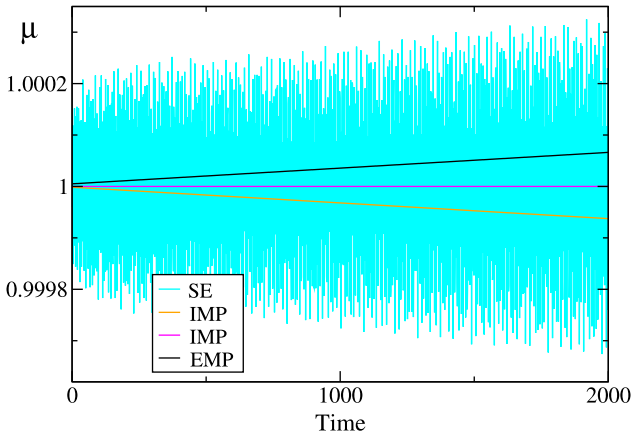

FIG. 2. Conservation of Lagrange multiplier μ for different integration schemes [Symplectic Euler (SE), Implicit Midpoint (IMP), Explicit Midpoint (EMP)] and $K = 0.5$. The orange and magenta curves differ in the convergence threshold in the nonlinear solver (10^{-6} and 10^{-12}).

We have integrated (11) with different integration schemes and compared the results for the symplectic Euler method, the implicit and the explicit midpoint method, as well as a 4th order explicit Runge-Kutta scheme applied to the old model (4). We used stepsize 0.002, transient time 100, and simulation time 5000. As illustrated in Fig. 2, on short time intervals, the different solvers deliver similar results for the multiplier μ. However, if we want its exact conservation, a geometric integrator like the implicit midpoint method should be applied with a sufficient accuracy for the nonlinear solver at every integration step. When the accuracy is not sufficient, the multiplier drifts from the value 1, as for the explicit midpoint method.

To understand the transition from the non-synchronized state for small K to synchronized state for large K, we performed sequences of simulations by increasing the parameter K with random initial conditions for $\{\theta_i\}$ and $\{\dot\theta_i\}$, for

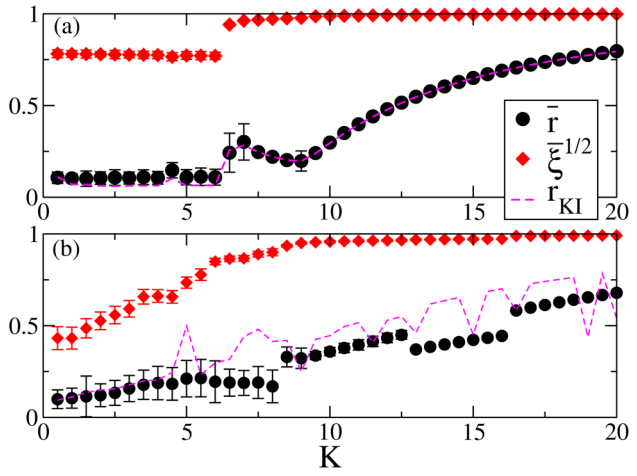

FIG. 3. Time-averaged order parameters vs coupling constant K, with (a) perfectly balanced bimodal δ-distribution or (b) Gaussian distributions of the Ω_j. r_{KI} is the average standard Kuramoto parameter, calculated via a 4th order Runge-Kutta scheme in the original formulation [i.e., via integrating Eq. (4)]. $\bar r$ and $\bar\xi^{1/2}$ are the average standard Kuramoto parameter and generalized order parameter, respectively, obtained with the implicit midpoint rule applied to the pHDAE formulation. The data have been obtained by changing adiabatically the coupling constant, starting from $K = 0$ and with $\Delta K = 0.5$.

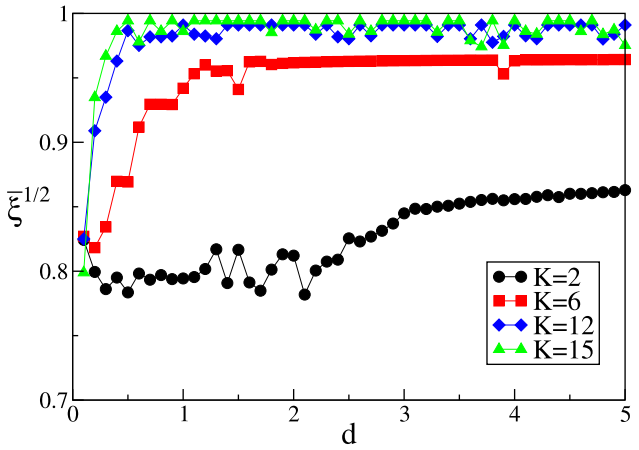

FIG. 4. Average order parameter $\bar{\xi}^{1/2}$ vs the damping constant d for different coupling constants K.

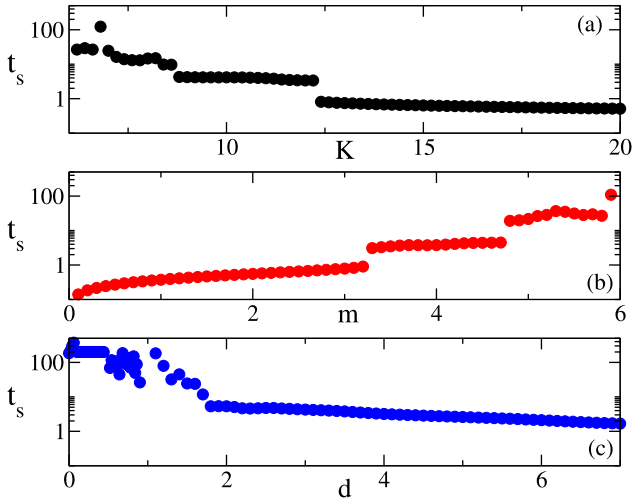

FIG. 5. Time t_s necessary to reach good synchronization ($\bar{\xi}^{1/2} > 0.95$), as a function of the parameters K, m, d, which represent the values to which the parameters are tuned initially in order to calculate the time needed to reach synchronization. To efficiently control the system, when stability is affected by emerging disturbances, it is more convenient to increase the coupling constant. On the other hand, bigger inertia prevents the system from fast synchronization recovery since it slows down the dynamics. t_s is expressed in nondimensional time units.

both (4) and (11). In each case, the simulation was initialized by employing the last values of the previous simulation. The average COP $\bar{r}$ and its GOP counterpart $\bar{\xi}^{1/2}$ (assuming $\xi(q) \geq 0$) both show a non-monotonic behavior in K, especially the former (see Fig. 3). For the bimodal δ-distributions [panel (a)] and small coupling values $\bar{r} \propto 1/\sqrt{N}$, we observe an abrupt jump for $K = 6.5$. Subsequently, $\bar{r}$ decreases, reaching a minimum at $K = 9$. For larger K, then $\bar{r}$ increases monotonically toward full synchronization. The generalized order parameter $\bar{\xi}^{1/2}$, on the other hand, does not show such an irregular behavior for small coupling values but has almost constant value until $K = 6.5$, where the transition to synchronization takes place and from then on rapidly increases toward 1. Since ξ takes into account the topology of the network, the analysis of the synchronization level is more stable for small coupling constants, while it is still able to identify the transition to synchronization at $K = 6.5$. The correctness of the critical value for the transition to synchronization can be confirmed indirectly by calculating the maximal Lyapunov exponent (see Ref. 23). The COP $\bar{r}$ fails in identifying the correct level of synchronization because, for $K < 6.5$, the system splits in two clusters: one consisting of the sources, oscillating close to their proper frequency, and one consisting of the consumers, which rotates with negative average velocity. This non-trivial form of partial synchronization already present in the network is not detected by $\bar{r}$, whose value around $1/\sqrt{N}$ indicates that the system behaves asynchronously. By increasing the coupling to $K \geq 7.5$, the two clusters merge into a single cluster, which is reflected in a monotonic increase of the average order parameters (see Ref. 23). For a bimodal Gaussian frequency distribution, the average order parameters $\bar{r}$, $\bar{\xi}^{1/2}$ as a function of the coupling constant reveal that, in this setup, it is more difficult to achieve synchronization, due to the inhomogeneity of the natural frequencies [see Fig. 3(b)]. Here, $\bar{r}$ is still irregular and unstable, irrespective of whether we use the original Kuramoto model with inertia or the pHDAE formulation, while $\bar{\xi}^{1/2}$ is stable and informative, with a continuous transition to synchronization, instead of a jump from partial to full synchronization. It should be noted that, while in these examples the pHDAE and the original formulation present similar qualitative behaviour [with a few noticeable differences in Fig. 3(b)], the discretization of the quadratic pHDAE with the implicit midpoint is usually more adequate in limiting situations.

We conclude this section by testing how adjusting the inertia m and the damping constant d could help with the synchronicity control of the system. For larger inertia, the critical coupling value for transition to synchronization increases, so that larger coupling strength is necessary to achieve the synchronized state; see also Ref. 23. On the other hand, for fixed K, larger damping constants d help reaching synchronization, as shown in Fig. 4. However, a consistent increase is possible only for K close to the critical value $K = 6.5$ as in Fig. 3, thus illustrating that the coupling strength plays a more important role in the transition than the damping constant. This effect is also observed when varying the mass m, while keeping K constant (see Ref. 23).

When a generator is diverging from the synchronized regime, it is important to react to this perturbation as fast as possible in order to avoid a shut-down of the generator. Starting from a slightly asynchronous model ($K = 6$), we can also control the time to synchronization t_s by changing K, d, or m; see Fig. 5. Adjusting mechanically some parameters of the system can thus be useful both to not drift away from synchronicity and to return to a synchronous state in a shorter time.

VI. CONCLUSIONS

We have presented a new port-Hamiltonian differential-algebraic formulation of the Kuramoto model of coupled rotators, as well as a new definition of the order parameter. The new pHDAE model formulation is structured in such a way that it can be easily extended to analogous pHDAE formulations of finer granularity as they are used in quantitative

stability and synchrony analysis of power systems. The new order parameter is more robust in limiting situations. We have also shown the advantage of the port-Hamiltonian formulation in the preservation of conserved quantities. Future work will include the analysis of the whole model hierarchy, whose lowest level is represented by the Kuramoto model with inertia described here.

ACKNOWLEDGMENTS

V.M. acknowledges support by Deutsche Forschungsgemeinschaft (DFG) via Project A2 of SFB 910 and *Einstein Foundation Berlin* via the Einstein Center ECMath. R.M. is supported by *Einstein Foundation Berlin* via the Einstein Center ECMath. S.O. and E.S. were supported by DFG via Project A1 of SFB 910.

[1] G. Filatrella, A. H. Nielsen, and N. F. Pedersen, Eur. Phys. J. B **61**, 485–491 (2008).
[2] P. Kundur, N. J. Balu, and M. G. Lauby, *Power System Stability and Control*, EPRI Power System Engineering Series (McGraw-Hill, 1994).
[3] S. Olmi, A. Navas, S. Boccaletti, and A. Torcini, Phys. Rev. E **90**, 042905 (2014).
[4] F. Salam, J. Marsden, and P. Varaiya, IEEE Trans. Circuits Syst. **8**, 673–688 (1984).
[5] T. Nishikawa and A. E. Motter, New J. Phys. **17**, 015012 (2015).
[6] M. Rohden, A. Sorge, M. Timme, and D. Witthaut, Phys. Rev. Lett. **6**, 064101 (2012).
[7] F. Doerfler, M. Chertkov, and F. Bullo, Proc. Natl. Acad. Sci. **6**, 2005–2010 (2013).
[8] N. Monshizadeh, C. De Persis, A. J. van der Schaft, and J. M. A. Scherpen, IEEE Trans. Automat. Control **63**, 1288–1299 (2018).
[9] A. J. van der Schaft and T. Stegink, "Perspectives in modeling for control of power networks," Annu. Rev. Control **41**, 119–132 (2016).
[10] A. Sarlette and R. Sepulchre, "Synchronization on the circle," in *The Complexity of Dynamical Systems: A Multi-disciplinary Perspective*, edited by J. Dubbeldam, K. Green, D. Lenstra, (Wiley, 2011), available at https://arxiv.org/pdf/0901.2408.pdf.
[11] R. Ortega, A. J. van der Schaft, Y. Mareels, and B. M. Maschke, Control Syst. Mag. **21**, 18–33 (2001).
[12] G. Golo, A. J. van der Schaft, P. C. Breedveld, and B. M. Maschke, *Nonlinear and Hybrid Systems in Automotive Control*, edited by A. Rantzer and R. Johansson (Springer, Heidelberg, 2003), pp. 351–372.
[13] A. J. van der Schaft, *Advanced Dynamics and Control of Structures and Machines* (Springer, New York, 2004), Vol. 444.
[14] P. C. Breedveld, *Modeling and Simulation of Dynamic Systems Using Bond Graphs* (EOLSS Publishers Co. Ltd./UNESCO, Oxford, UK, 2008).
[15] A. J. van der Schaft, *Surveys in Differential-Algebraic Equations I* (Springer, Berlin, 2013), pp. 173–226.
[16] C. Beattie, V. Mehrmann, H. Xu, and H. Zwart, preprint arXiv:1705.09081 (2017).
[17] C. I. Byrnes, A. Isidori, and J. C. Willems, IEEE Trans. Automat. Control **36**, 1228–1240 (1991).
[18] J. Cervera, A. J. van der Schaft, and A. Baños, Automatica **43**, 212–225 (2007).
[19] S. Gugercin, R. V. Polyuga, C. Beattie, and A. J. van der Schaft, Automatica **48**, 1963–1974 (2012).
[20] S. Fiaz, D. Zonetti, R. Ortega, J. M. A. Scherpen, and A. J. van der Schaft, Eur. J. Control **19**, 477–485 (2013).
[21] P. Monshizadeh, C. De Persis, N. van der Monshizadeh, and A. J. Schaft, in *2016 IEEE 55th Conference on Decision and Control (CDC)* (IEEE, 2016), pp. 4116–4121.
[22] M. Schröder, M. Timme, and D. Witthaut, Chaos: Interdiscip. J. Nonlinear Sci. **27**(7), 073119 (2017).
[23] V. Mehrmann, R. Morandin, S. Olmi, and E. Schöll, preprint arXiv:1712.03160 (2017).
[24] L. Brugnano and F. Iavernaro, *Line Integral Methods for Conservative Problems* (Chapman & Hall, 2015).
[25] P. Kunkel and V. Mehrmann, *Differential-Algebraic Equations: Analysis and Numerical Solution* (EMS Publishing House, Zürich, 2006).
[26] L. Fortuna, M. Frasca, and A. Sarra Fiore, Int. J. Modern Phys. **26**, 25 (2012).